THE JOURNAL OF BIOLOGICAL CHEMISTRY
Vol. 276, No. 52, Issue of December 28, pp. 49275–49282, 2001

Printed in U.S.A.

Regulation of Glycosaminoglycan Function by Osmotic Potentials

MEASUREMENT OF WATER TRANSFER DURING ANTITHROMBIN ACTIVATION BY HEPARIN*

Received for publication, May 15, 2001, and in revised form, October 18, 2001
Published, JBC Papers in Press, October 24, 2001, DOI 10.1074/jbc.M104413200

Maria P. McGee‡§ and Jie Liang¶

From the ‡Internal Medicine Department, Wake Forest University School of Medicine, Winston-Salem, North Carolina 27157 and the ¶Bioengineering Department, University of Illinois, Chicago, Illinois 60607

The sulfated glycosaminoglycan heparin is an important anticoagulant, widely used to treat and to prevent arterial thrombosis. Heparin triggers conformational changes in, and the functional activation of, the serine proteinase inhibitor antithrombin. We investigated water-transfer reactions during the activation process to explore the possibility that functional interaction between antithrombin and sulfated glycosaminoglycans can be regulated by osmotic potentials. Volume of water transferred upon heparin binding was measured from differences in free energy change, $\Delta(\Delta G)$, with osmotic stress, π. Osmotic stress was induced with chemically inert probes that are geometrically excluded from the water-permeable spaces of antithrombin and from intermolecular spaces formed during the association reaction. The free energy change, ΔG, for the antithrombin/heparin interaction was calculated from the dissociation constant, determined by functional titrations of heparin with antithrombin at fixed concentrations of the coagulation protease factor Xa. The effect of osmotic stress was independent of the chemical nature of osmotic probes but correlated with their radius up to radius >17 Å. In mixtures including a large and a small probe, the effect of the large probe was not modified by the small probe added at a large molar excess. With an osmotic probe of 4-Å radius, the $\Delta(\Delta G)/\pi$ slope corresponds to a transfer of 119 ± 25 water molecules to bulk solution on formation of the complex. Analytical characterization of water-permeable volumes in x-ray-derived bound and free antithrombin structures revealed complex surfaces with smaller hydration volumes in the bound relative to the free conformation. The residue distribution in, and atomic composition of, the pockets containing atoms from residues implicated in heparin binding were distinct in the bound *versus* free conformer. The results demonstrate that the heparin/antithrombin interaction is linked to net water transfer and, therefore, can be regulated in biological gels by osmotic potentials.

Antithrombin is one of the more important inhibitors of blood coagulation proteinases. Deficiencies in antithrombin, either acquired or congenital, are associated with thrombosis. The inhibitory activity of antithrombin is markedly increased by binding with charged glycosaminoglycans (GAGs)[1] present on the vascular wall and extravascular spaces (1–8). Among GAGs, the heparan sulfates are the most effective antithrombin activators. Stereospecific requirements for maximal inhibitory activity have been ascribed to a pentasaccharide sequence containing four sulfate groups on glucosamine residues and two carboxylates on uronic acid residues (9, 10). Commercial preparations of heparin used routinely as anticoagulants are enriched with these highly charged sequences as compared with heparan chains that are isolated from the vasculature (11). *In vivo*, natural antithrombin ligand(s) are part of complex biopolymer gels and subjected to hydration and dehydration osmotic forces (12) in the extracellular matrix. The possible effect of osmotic forces on the functional interactions of GAGs remains essentially unexplored. In the present study, we examine the effect of osmotic forces on the heparin/antithrombin interaction.

Antithrombin is a prototype metastable protein, and its activation by heparin appears to result from the release of several structural constraints (6, 7, 13, 14). Considerable evidence indicates that antithrombin undergoes sequential changes in conformation during functional interactions with heparin and its target proteinases (2–4). The conformational changes initiated by heparin propagate throughout the antithrombin structure in ways that are not completely understood. Kinetically, it has been shown that the antithrombin/heparin interaction is a two-step reaction with a strong electrostatic component. An initial, low affinity step equilibrates very rapidly and induces the conformational transitions leading to high affinity interactions (8, 14). These antithrombin conformational transitions improve access of the reactive loop to the target proteinase's active site and are responsible for most of the ~500-fold increase in antithrombin affinity for coagulation factor Xa (fXa) (1, 7, 13). The subsequent inhibition of fXa is also a two-step process (3, 5–8, 13–18), with an initial fast equilibrating step to form a ternary complex, followed by a slower, first-order reaction resulting in heparin release and formation of an essentially irreversible antithrombin-fXa complex. Proteinase inhibition and heparin release are linked to reinsertion of antithrombin's reactive loop into a β-sheet structure in the protein's core and translocation of the proteinase from its initial low affinity interaction site in the exposed reactive loop to the other end of the antithrombin molecule (5, 6).

Previous studies using the osmotic stress (OS) technique indicated that the first-order reaction leading to irreversible antithrombin-fXa complex formation is linked to net water transfer from the reactants to bulk solution (19). The possibil-

* This work was supported by National Science Foundation Grant MCB-9601411 and National Institutes of Health Grant HL57936; computational geometry aspects were supported in part by National Science Foundation Grant MCB998008 (to J. L.). The costs of publication of this article were defrayed in part by the payment of page charges. This article must therefore be hereby marked "*advertisement*" in accordance with 18 U.S.C. Section 1734 solely to indicate this fact.

§ To whom correspondence should be addressed: Internal Medicine Dept., Wake Forest University School of Medicine, Medical Center Blvd., Winston-Salem, NC 27157. Tel.: 336-716-6716; Fax: 336-716-9821; E-mail address: mmcgee@wfubmc.edu.

[1] The abbreviations used are: GAG, glycosaminoglycan; PEG, polyethylene glycol; OS, osmotic stress; fXa, factor Xa; H, heparin; AT, antithrombin; B, bound; F, free; PDB, Protein Data Bank; atm, atmosphere(s).

ity that hydration water is transferred during heparin-induced conformational transitions has not been investigated before. The theoretical basis of the OS technique has been described and validated in detail (20–26) and revised recently (27). Osmotic stress gives a direct thermodynamic measure of hydration. Many functional reactions of complex proteins like antithrombin are associated with conformational transitions that drastically alter the magnitude and distribution of their water-permeable spaces (19–26). During these transitions, the change in free energy has a component corresponding to the work of water transfer. When the transition proceed in the presence of cosolutes that are excluded from the water-permeable spaces, the difference in water activity between the excluded spaces and bulk solution favor water transfer to bulk solution. The sensitivity of the free energy change, (ΔG), to water activity is a measure of the volume of water transferred during the transition and reflects differences in hydration between initial and final states. In the present work, OS is used with functional titrations to analyze antithrombin activation by heparin. Results show net water transfer from reactants to bulk on formation of the heparin-antithrombin complex and imply that functional GAG interactions are susceptible to osmotic regulation *in vivo*.

MATERIALS AND METHODS

Determination of Functional Binding Parameters—The dissociation constant of the heparin/antithrombin interaction was determined from functional titrations under different osmotic stress conditions. The effect of osmotic stress on binding parameters was analyzed on the basis of the previously validated (18) kinetic scheme.

$$\mathrm{AT} + \mathrm{H} \overset{K_h}{\longleftrightarrow} \mathrm{AT{\cdot}H} + \mathrm{fXa} \overset{K_t}{\longleftrightarrow} \mathrm{H{\cdot}AT\text{-}fXa} \overset{k}{\rightarrow} \mathrm{AT\text{-}fXa} + \mathrm{H}$$

REACTION 1

K_h is the equilibrium dissociation constant for the antithrombin/heparin interaction (AT·H). K_t is the dissociation constant for the ternary interaction between fXa and the AT·H complex, and k is the first-order rate constant for the stabilization of the inhibitory complex.

The observed pseudo-first-order rate constant, k_{obs}, is a hyperbolic function of the AT·H complex concentration.

$$k_{obs} = k[\mathrm{AT{\cdot}H}]/(K_t + [\mathrm{AT{\cdot}H}]) \qquad \text{(Eq. 1)}$$

The stabilization of the complex is closely linked to the release of heparin. Although the mechanism that links heparin dissociation to the first-order stabilizing step is not clear, detailed kinetic analyses indicate that dissociation occurs either simultaneously or in a faster, subsequent step (18, 28, 29).

Functional Saturation Curves—Functional titration experiments were performed within a concentration range of antithrombin (20–450 nM), giving K_t [tmt] [AT·H] and $k_{obs} = k$ [AT·H]/K_t, and at fixed and low heparin (20 nM) and fXa (10 nM). Under these conditions, the change in k_{obs} with antithrombin concentration reflects the concentration of AT·H and follows the saturation curve of heparin with antithrombin (18) from which a functionally determined dissociation constant, K_d, can be determined.

Antithrombin and heparin were equilibrated in Tris buffer, 25 mM, pH 7.2–7.4 at 25 °C, with NaCl at either 0.075 or 0.2 N. Osmotic stress was induced with the following chemically inert cosolutes: polyethylene glycol, M_r 300 or 8000 (PEG 300 or 8000); dextran, M_r 10,000; or polyvinylpyrrolidone, M_r 40,000. Standard and "stressed" solutions were identical in all components except for the added cosolute. The difference in osmotic pressure generated by the added cosolute was determined from empirical relationships derived by direct osmotic pressure measurements (24, 25). The change in [AT·H] with antithrombin was determined from the exponential rate, k_{obs}, of fXa activity decay. The fXa activity was measured in six sequential samples withdrawn from reaction mixtures at 5–50-s intervals and diluted immediately in hexamethrine bromide (100 μg/ml). Residual protease activity was determined from the initial rate of substrate hydrolysis (methoxycarbonyl-D-cyclohexylglycylarginine-*p*-nitroanilide acetate), as described previously (32). In reaction mixtures without heparin or without antithrombin, the fXa activity did not change significantly during the reaction time.

Stoichiometry—The possible effect of OS on the [AT·H]/fXa stoichiometry and changes in proportions of antithrombin branching into the substrate pathway was also investigated. In these experiments, antithrombin and fXa were incubated at various molar ratios with heparin at fixed concentration. Reactions were followed under either standard or OS conditions until completion. The stoichiometry was calculated as the abscissa intercept of linear regression plots of residual proteinase activity *versus* the antithrombin/fXa ratio (18).

Miscellaneous Procedures—The quadratic form of the binding equation was fitted to data points (18), using the computer program TableCurve (SAS Institute, Inc., Cary, NC), and linear regression analyses were performed with the computer program Stat-View (SAS Institute, Inc., Cary, NC.). Commercial-grade heparin with average molecular weight of ~17,000 was purchased from Sigma. Fractionated heparin (molecular weight of 3000) and human antithrombin and factor Xa were purchased from Enzyme Research Laboratories.

Determination of Water Transfer during Antithrombin/Heparin Interactions and Theoretical Considerations—Experimentally, the possibility that a particular interaction is associated with net water transfer is determined from the difference in free energy change $\Delta(\Delta G)$ with osmotic pressure. The direction of the water transfer is also deduced from the $\Delta(\Delta G)/\pi$ slope. The slope is positive when transfer is from bulk to reactants. The slope is negative when transfer is from reactants to bulk. Changes in free energy are calculated from the binding parameters according to classical thermodynamic principles (33).

Osmotic stress theory (20–27) is derived from the theory of dilute solutions (34, 35), as it explains the indirect effects of cosolutes on macromolecules. It focuses on the role of hydration water in the region within and around a macromolecule from which cosolutes, but not water, are excluded. Detailed commentaries on various cosolute effects, such as crowding, preferential hydration, and binding, have been published (27). Here we summarize the theory only in relation to the antithrombin activation experiments we present.

To analyze the antithrombin transformation between an F (heparin-free) and an B (inhibitory, heparin-bound) state, the osmotic stress technique can give a thermodynamic measurement of the hydration volume difference.

The free energy difference from F to B is the free energy difference, ΔG between the bound (G_B) and unbound forms of antithrombin (G_a) and heparin (G_h).

$$\Delta G = (G_a + G_h) - G_B \qquad \text{(Eq. 2)}$$

and

$$\Delta G = -RT \ln K \qquad \text{(Eq. 3)}$$

K is a parameter measuring the ratio between the concentrations (or probabilities) of states F and B at equilibrium, R is the gas constant (1.987 cal/mol/degree), and T is the temperature (degrees Kelvin). The volume of water transfer is calculated from the equivalence: 1 atm × (volume of 1 mol of water) = 0.435 cal/mol. Thus, from the measured ratio $\Delta(\Delta G)/\pi$, (cal/mol/atm)/0.435 = mol H_2O.

In a multicomponent solution, such as those used to determine equilibrium parameters, the colligative properties, including the osmotic pressure, depend on the activity of all components. In our osmotic stress experiments, the activity of all components was held constant except for water and the inert cosolute used to induce osmotic stress. The composition of stressed and standard solutions was identical except for incremental additions of cosolute. The antithrombin and heparin molecules in the diluted solution used to measure equilibrium parameters are expected to influence the composition of the region of solution close to their surface, or *sphere of influence* (27, 34, 35). Focusing on the inert cosolute and the water within the antithrombin's sphere of influence, the solution will have N_w, and N_c, molecules of water and cosolute, respectively, whereas in regions outside the sphere of influence the solution will have n_w and n_c molecules, respectively. Obviously, the sphere of influence includes all geometrical spaces within and near antithrombin, from which the cosolute is sterically excluded. However, following thermodynamic reasoning, the size of the sphere of influence is of no importance, because the osmotic stress on the molecule depends on the disproportion of cosolute and water within and outside the sphere (25).

The Gibbs-Duhem (34) equation links the changes in chemical potential, $d\mu$, within the antithrombin sphere of influence,

$$\mathrm{d}\mu_a = -N_w \mathrm{d}\mu_w - N_c \mathrm{d}\mu_c, \qquad \text{(Eq. 4)}$$

and at solution regions outside the antithrombin's sphere of influence,

$$n_w d\mu_w + n_c d\mu_c = 0. \quad \text{(Eq. 5)}$$

These relations express the fact that the changes in cosolute, $d\mu_c$, and water, $d\mu_w$, chemical potentials are directly linked. The same arguments apply to the chemical potential of heparin. The change in water's chemical potential can also be expressed by considering the change in osmotic pressure induced by cosolute.

$$d\mu_w = -V_w d\pi \quad \text{(Eq. 6)}$$

V_w is the molecular volume of water, and $d\pi$ is the change in osmotic pressure induced by changes in cosolute concentration (34, 35).

The change in chemical potential is closely related to Gibbs free energy and can be defined as the Gibbs free energy per molecule. This definition of the free energy is frequently used in utilitarian forms of the Second Law equation, and its derivation is based on Euler identity for homogeneous functions (34). From Equations 2–6 above, we obtain Equation 7.

$$d\Delta G = -\Delta N_{ew} d\mu_w \quad \text{(Eq. 7)}$$

N_{ew} is the excess (or deficit) amount of water in regions within, as compared with outside, antithrombin's sphere of influence (27). If N_{ew} differs in the F and B states, then the change in the equilibrium parameter upon incremental additions of cosolute measures the water molecules transferred in going between the F and B state, as shown in Equations 8 and 9.

$$\Delta N_{ew}^{FB} = N_{ew}^{F} - N_{ew}^{B} \quad \text{(Eq. 8)}$$

and

$$d(\Delta G_{FB})/d\pi = N_{ew}^{FB} V_w \quad \text{(Eq. 9)}$$

Therefore, the slope of the difference in free energy change (determined from changes in equilibrium constant) with osmotic pressure gives the amount of water transferred as reactants go from the F to the B state.

On the basis of transition-state theory (33), differences in the changes in free energy of activation with osmotic pressure can also be used to measure hydration volume changes. In this case, thermodynamic reasoning is applied to the formation of the activated complex, and the equilibrium considered is between the reactants and the activated complex. This activated complex corresponds to an intermediate transient conformation, the hydration of which is likely to differ from that of both the initial and final states. Therefore, it is not useful to correlate volumes with x-ray-derived structures, which are probably more closely related to the initial and final states. However, because rate measurements are much more sensitive than equilibrium constant determinations, the difference in the free energy of activation change is useful in detecting other possible secondary effects of cosolutes that are not osmotic.

Calculation of Water-permeable Spaces in AT Structure—Water-permeable spaces excluded by the osmotic probes in antithrombin were analyzed from x-ray-derived structures of bound and free antithrombin using CAST software (36, 37). CAST is a unique computational method that provides comprehensive identification and accurate measurement of surface concavities of various shapes and geometries. It implements algorithms, developed using analytical computational geometry, and formalizes intuitive notions to classify concave regions into voids, pockets, and depressions. Briefly, voids are completely buried without access to the outside. Pockets are connected to the outside through a constricted mouth opening and mouth openings connecting the inside of a concave pocket with bulk solvent spaces are defined unambiguously using a triangulation procedure. All pockets and voids on a protein are identified and their metric properties, including both the pocket and mouth, determined analytically. The location of all pockets and voids, their atomic composition, volume, and the area of the mouths collectively describe the shape and specific physicochemical environment of a protein, providing a unique hydration fingerprint for each protein structure.

Hydration fingerprints of antithrombin conformers were calculated from x-ray-derived atomic coordinates in the Brookhaven Protein Data Bank files 2ant (30) and 1azx (29). The general characteristics of these structures and their putative functional significance have been considered previously (29–31). The 2ant file includes atomic coordinates of antithrombin in an L (latent) and I (inhibitory) conformation in the absence of ligand. In the L conformer, the reactive loop is fully inserted as strand 4 of β-sheet A, whereas in the I conformer, the reactive loop is partially inserted. The 1azx file includes the coordinates of the same two conformers bound to an oversulfated heparin analog, pentasaccharide. In this structure, the reactive loop of the I conformer is not inserted.

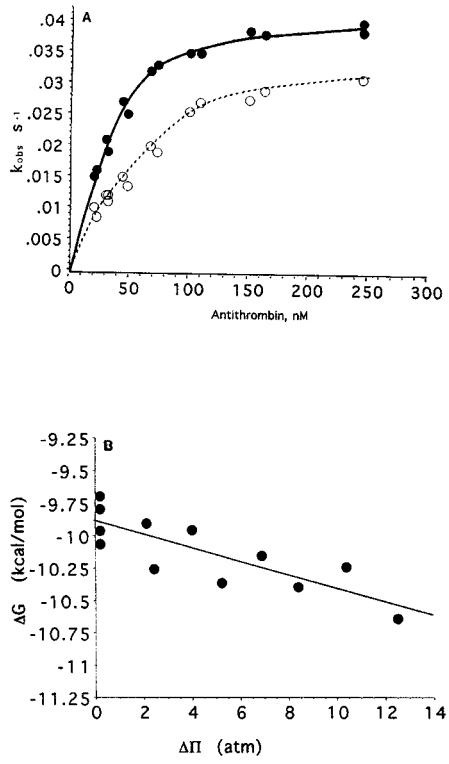

FIG. 1. **Titration of heparin with antithrombin under osmotic stress.** *A*, heparin at a fixed concentration, 20 nM, was equilibrated with antithrombin at concentrations ranging from 0 to 300 nM. At each antithrombin concentration, the fraction of total heparin in antithrombin-heparin complexes was determined by measuring the exponential decay rate in fXa activity added at 10 nM. ○, standards were in Tris buffered at pH 7.2–7.4 with NaCl at 0.2 N. ●, stressed solutions were identical but included PEG 300 at a concentration of 10% weight. *B*, the difference in free energy change with pressure was calculated from K_d values determined in titrations at different OS levels. The osmotic pressure difference, $\Delta\pi$, was calculated from empirical relationships derived using direct osmotic pressure measurements (25, 45).

The water-permeable pockets stressed by PEG 300 were defined in the structures as pockets with mouth areas $< \pi$ (4 Å)^2. The section of PEG 300 was modeled from a sphere of 4-Å radius. This value is an average of several similar values available in the literature (39–41). For CAST calculations, the structures were prepared by separating the I and L conformers and removing the pentasaccharide manually. Pocket structures corresponding to the heparin-binding region were defined as those containing atoms from residues demonstrated previously to be important in heparin binding by mutational analyses (15, 29). Residues used in the search were Lys^{11}, Arg^{13}, Arg^{24}, Arg^{47}, Lys^{125}, Arg^{129}, Arg^{145}, Glu^{113}, Arg^{132}, Arg^{133}, and Arg^{136}.

RESULTS

Changes in Binding Parameters with Osmotic Stress—The possibility that net water transfer is linked to antithrombin activation by heparin was investigated using functional titration and OS technique. Binding parameters were determined by titration of 20 nM heparin with 0–350 nM antithrombin in 25 mM Tris buffer, 0.2 N NaCl, pH 7.4, at 25 °C. The fraction of bound heparin was determined as a function of antithrombin concentration from the exponential rate of fXa inhibition. The rate, k_{obs}, increased with antithrombin concentration approaching asymptotically to a maximum (Fig. 1*A*). Parameters K_d and V_{sat} (k_{obs} at saturation) were determined by fitting the quadratic form of the binding equation to data. In titrations with PEG 300, ~4-Å radius, the dissociation constant decreased significantly, indicating water transfer from reactants

TABLE I

Water transfer measured by OS with polymers of different sizes and chemical structure

The value of K_d was determined as indicated in the legend to Fig. 1. The osmotic probes were present at concentrations of 5–8% wt. Osmotic pressure differences between standard and stressed solutions (*i.e.* with the OS probes) were calculated using empirical relationships derived from direct osmotic pressure measurements (24, 25, 45). Molecular masses indicated are the average values provided by suppliers. The values indicated for the probe radius correspond to published values of the radius of gyration derived from gel-filtration experiments (38). For PEG 300, the value used is the average of several published values (39–41). The number of water molecules transferred from excluded spaces to bulk solution during the interaction was determined from the thermodynamic equivalence, volume of 1 mol of water = 0.435 cal/mol/atm. The $\Delta(\Delta G)/\pi$ values are mean and standard errors from three to six determinations.

OS probe	M_r	Radius	K_d		$\Delta(\Delta G)/\pi$	Net transfer
			Standard	Stressed		
		Å	nM		*cal/mol/atm*	*mol H_2O*
PEG:	300	4	68.4 ± 7.5	22.4 ± 3.8	−51.6 ± 9	107 ± 18
	600	7	51.2 ± 0.1	20.4 ± 7.5	−118 ± 39	271 ± 88
	3000	17	58.5 ± 5.9	18.0 ± 5.6	−782 ± 68	1798 ± 157
	8000	26	62.8 ± 2.8	15.6 ± 2.7	−871 ± 79	2002 ± 187
Dextran	10,000	24	68.5 ± 2.8	30.6 ± 3.6	−943 ± 169	2149 ± 402
PVP[a]	40,000	NA	56.3 ± 2.1	19.1 ± 2.0	−718 ± 92	1652 ± 212

[a] Polyvinylpyrrolidone.

to bulk solution on formation of the antithrombin-heparin complex. The free energy change for the interaction decreased linearly with OS, and the slope, $\Delta(\Delta G)/\pi$, was 52 ± 11 corresponding to a transfer of 119 ± 25 water molecules on formation of the complex (Fig. 1*B*).

Effect of Osmotic Probe Size—To explore the size of volumes formed between antithrombin and heparin during activation, titration experiments were repeated, using polymers of various sizes to induce OS. With all probes, the dissociation constant decreased, and the volume measured was correlated to probe size for probes with radii between 4 and 17 Å up to a maximum of ~2000 molecules of water (Table I).

Effect Induced with Chemically Different Probes—Titrations were repeated in solutions stressed with probes having physicochemical properties different from PEG. Results indicate that the effect was independent of the chemical nature of the osmotic probe. Normalized relative to osmotic pressure, the magnitude of changes in binding parameters measured in reactions stressed with polymers of either dextran or polyvinylpyrrolidone were not significantly different from those measured with the polyethylene glycols (Table I). These findings exclude the possibility that the observed decrease in K_d reflects specific molecular interactions between the PEG probes and reactants.

Effect of Salt Concentration on Parameters Measured under OS—For these comparative experiments, functional binding parameters were measured in two sets of reaction mixtures that were identical except for the NaCl concentration that was at either 0.075 or 0.2 N. Decreasing the salt concentration in nonstressed control solutions resulted in significantly lower K_d values. In contrast, the V_{sat} was essentially independent of ionic strength (Table II), which should be expected from the known dependence of the heparin/antithrombin association rate on electrostatic forces. Measured from this base line, OS with small probes did not decrease but rather slightly increased K_d values. When induced with large probes, OS increased K_d values by severalfold relative to the baseline values measured at low ionic strength (Table II). These results indicate that osmotic stress and ionic strength influence the same initial step of the antithrombin/heparin interaction. The differences between small and large probes are consistent with additional OS effects on subsequent reaction steps.

Effect of OS on Stoichiometry—The stoichiometry of antithrombin/fXa interaction did not change significantly with OS when measured either at high or low ionic strength. The stoichiometry determined in reaction mixtures with 0.2 N NaCl was 1.26 ± 0.03 *versus* 1.23 ± 0.05 in stressed and nonstressed reactions, whereas the stoichiometry measured in reaction mixtures with 0.075 N NaCl was 1.29 ± 0.11 and 1.21 ± 0.04 in stressed and nonstressed solutions, respectively. These results also exclude the possibility that osmotic stress at either low or high ionic strength induced aggregation or precipitation of reactants.

Reaction Rates in Solutions Stressed Simultaneously with Large and Small Osmotic Probes—Experiments were designed to test the possibility that the differential effect observed with large and small PEG probes at high and low ionic strength reflects causes other that osmotic. Because rate measurements are much more sensitive than K_d determinations, they were used to test for secondary effects. For these experiments, reaction mixtures contained heparin at 40 nM and fXa 10 nM in Tris buffer, pH 7.4, with NaCl at 0.075 N with antithrombin at 100 nM. Antithrombin concentration was chosen on the basis of titration experiments indicating, that under these conditions, the dissociation constant in the presence of large probes is 99.0 ± 7.7 nM. Therefore, at antithrombin concentrations near this K_d value, changes in either K_d or V_{sat} are reflected in the pseudo-first-order rate constant, k_{obs}.

Reaction rates were measured in two sets of reaction mixtures, each set including six different probe concentrations. One set, with PEG 3400 at 0–5%, corresponded approximately to a 0–16 10^{-3} M concentration range and to a 0–0.7646 atm pressure range. The other set had identical concentrations of PEG 3400 but, in addition, contained 8.5% PEG, corresponding to ~28 10^{-2} M and to a pressure of 8.5 atm. The change in free energy of activation was determined from the relationship (33), shown in Equation 10.

$$\Delta G\ddagger = -RT \ln kh/k_B T \qquad \text{(Eq. 10)}$$

k is the rate (s^{-1}), R is the gas constant (1.987 cal/mol/degree), T is the temperature (degrees Kelvin), h is Plank's constant (1.584×10^{-34} cal s^{-1}), and k_B is Boltzmann's constant (3.29×10^{-24} cal/degree). The difference in the free energy of activation change induced with PEG 3400 in the presence or absence of PEG 300 is shown in Fig. 2*A*. At molar excesses of over 20-fold, the small PEG probe did not influence the effect measured with the larger probe (Fig. 2*B*). This confirms that the difference between effects observed with large and small probes reflects primarily the size of the geometrical volumes excluded by each. Results also indicate that changes in the dielectric constant and or viscosity of solutions do not influence the $\Delta(\Delta G)/\pi$ slope. These results further exclude the possibility that the effects observed are the result of direct binding interactions between the PEG probe and the reactants.

Osmotic Stress Effects in Reactions with Fractionated Hepa-

TABLE II

Functional titrations under osmotic stress: effect of ionic strength and probe size

Heparin at a fixed concentration of 20 nM was titrated with 40–300 nM antithrombin in either standard solutions or solutions containing OS probes of the indicated radius size and NaCl at the indicated concentration. The probes were PEG 300 and PEG 8000 at 10 and 8% wt, respectively. The fraction of heparin bound as a function of antithrombin concentration was determined from the exponential decay rate of fXa activity added at a fixed 10 nM concentration to preequilibrated antithrombin-heparin solutions. The rate in standard and stressed solutions was measured in parallel reaction mixtures at the same dilutions. Parameters K_d and V_{sat} were calculated by fitting the quadratic form of the binding equation to rate/concentration data points (24).

Radii[a]	NaCl	K_d		V_{sat}		Second-order rate coefficient[b]	
		Standard	Stressed	Standard	Stressed	Standard	Stressed
Å		nM		$s^{-1} \times 10^3$		$\mu M^{-1}\ s^{-1}$	
4	0.20	67.8 ± 5.3	23.6 ± 2.9	42 ± 3	46 ± 4	2.1 ± 0.2	2.3 ± 0.2
4	0.075	17.2 ± 2.0	21.6 ± 5.0	44 ± 5	60 ± 7	2.2 ± 0.1	3.0 ± 0.4
26	0.20	62.7 ± 2.8	15.7 ± 2.7	36 ± 6	91 ± 5	1.8 ± 0.3	4.5 ± 0.3
26	0.075	17.2 ± 2.9	33.1 ± 5.4	49 ± 4	109 ± 4	2.4 ± 0.2	5.4 ± 0.2

[a] The radii of the OS probes are from published values (38–41).

[b] Second-order rate coefficients for the formation of the ternary H · AT-fXa complex were calculated from the V_{sat} and the concentration of AT · H at saturation.

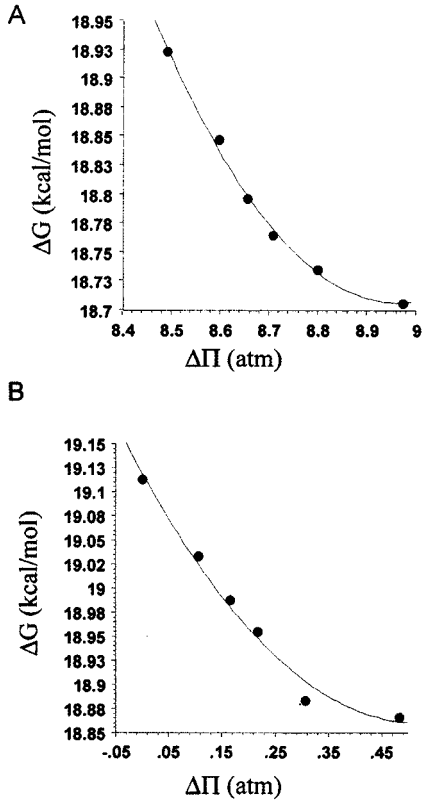

FIG. 2. **Osmotic stress effects of large and small probes in mixed solution.** The change in free energy of activation was evaluated from the first-order rate constant, determined in reaction mixtures stressed with either PEG 3400 and PEG 300 (*A*) or PEG 3400 alone (*B*). Data in *panel A* are from experiments where the PEG 300 concentration was fixed at 0.26 M, whereas PEG 3400 concentration ranged from 0 to 0.016 M. Data in *panel B* are from experiments with only PEG 3400 at 0–0.016 M. Reaction mixtures included 100 nM antithrombin, 40 nM heparin, and 10 nM fXa in 25 mM Tris, pH 7.2, with 0.2 N NaCl. The initial slopes determined from the first coefficient of a second degree polynomial fitted to data points were 0.959 ± 0.2 and 0.991 ± 0.11 cal/mol/atm, and not significantly different, in *A versus B*, respectively.

rin—To determine the possible effects of heparin heterogeneity, fractionated and unfractionated heparin preparations were used in parallel osmotic stress experiments. For these experiments, reaction mixtures were stressed with PEG 8000 in buffer solutions containing 0.075 N NaCl. Heparin concentration was fixed at close to the K_d value: 2 μM and 20 nM for fractionated and unfractionated preparations, respectively. The osmotic effect determined from reaction rates was 688 ± 6.7 and 653 ± 57 cal/mol/atm in mixtures with fractionated and commercial-grade heparin, respectively. These two values are the mean and standard deviation obtained from three different rate determinations, and their difference is not statistically significant. This observation indicates that heparin heterogeneity is not likely to influence the results of osmotic stress experiments.

Water-permeable Spaces in X-ray-derived Antithrombin Structures—Previous structural analyses of x-ray-derived antithrombin models identified differences between structures believed to represent conformations with high and low affinity for heparin. In particular, the redistribution of positively charged residues and dissipation of the surface charge density in the heparin binding region was correlated with low heparin affinity (30). Our results using OS suggest additional structural correlations on the basis of volume differences. The link between water transfer to bulk and formation of the antithrombin-heparin complex predicts smaller hydration volumes in bound *versus* free antithrombin. To explore this prediction and to gain further insight into the functional significance of antithrombin structures, the water-permeable spaces in x-ray-derived models were computed analytically, using CAST software (36, 37). Water was modeled as a spherical probe of 1.4-Å radius (Fig. 3*A*). The four conformers analyzed (2ant I, 1azx I, 2ant L, and 1azx L) had very complex surface structures composed of 70, 66, 53, and 59 distinct water permeable pockets, respectively. The location, atomic composition, and metric characteristics of the water-permeable pockets differed among conformers, particularly at the heparin-binding region. The heparin pockets were identified as those containing atoms from residues Lys^{11}, Arg^{13}, Arg^{24}, Arg^{47}, Lys^{125}, Arg^{129}, Arg^{132}, and Arg^{145}, previously implicated in heparin binding by mutational analyses (15). Total volumes in the structures and in pockets with atoms from heparin-binding residues in 1azx I and 2ant I conformers are listed in Tables III and IV. The surface of the heparin-binding region includes eight distinct pockets. This topological complexity indicates that shape complementarity between the ligand and the receptor surfaces contributes to the interaction's specificity (Fig. 3*B*). The volume of the pockets in the heparin-binding region, measured after removing the pentasaccharide, was significantly larger in the 1azx I than in the 2ant I conformer. Analysis of the surface structure of the 1azx I conformer with the pentasaccharide analog in place indicated a very close fit of the ligand in the pockets. This observation suggests that the excess volume measured in the unoccupied heparin-binding site is largely displaced upon binding. However, the volumes displaced by heparin cannot be calculated from the available bound structure, as the ligand pentasaccharide is smaller and occupies only a fraction of the known heparin-binding region (29, 15). An estimate of the total volume

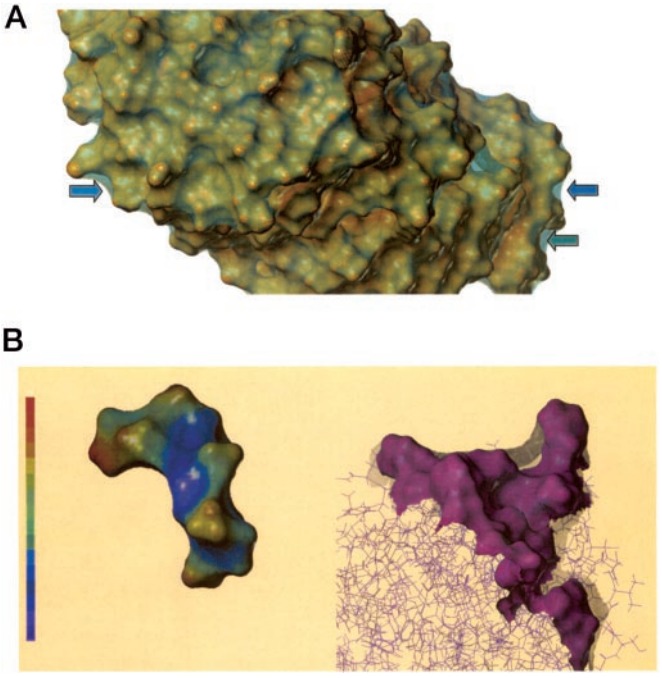

FIG. 3. **Spaces in the antithrombin structure permeable to water but inaccessible to osmotic probes with 4-Å radius.** *A*, the molecular surface of antithrombin was generated from the x-ray-derived structure of conformer I in PDB file 1azx. The surface generated with a spherical probe of 4 Å radius (*blue*) was superimposed on the water-accessible surface generated with a 1.4 Å radius probe (*yellow/orange*). The difference between volumes bounded by the two surfaces represents volumes inaccessible to the probe. These spaces, distributed throughout the antithrombin structure, are subjected to OS in solutions containing cosolutes with radius ≥ 4 Å. *Arrows* point to some of these surface pockets seen in profile. *B*, detail of the surface in the heparin-binding region of 1azx I (*right*) and of the electrostatic potential surface of the ligand (*left*). The surface accessible to water within a 6-Å distance from the ligand but excluding the ligand is rendered in *purple*, whereas the surface accessible to water and PEG 300 is rendered in *gray*. The background structure is a line rendition of bonds in 1azx I. The electrostatic potential on the ligand was mapped to its water-accessible surface after calculating charges using the Gasteiger-Huckel method implemented with Sybyl. The more electronegative regions are *darker blue*. The ligand is an oversulfated analog of the heparin pentasaccharide sequence and induces maximal antithrombin activity in functional assays. Surfaces were calculated by the Connolly method (42) implemented with MOLCAD, assigning a radius of 1.4 Å to the water probe.

TABLE III

Volumes of pockets found in different antithrombin conformers

The volume of pockets in four different x-ray-derived antithrombin structures were identified and measured using α-shape-based analytical computational geometry implemented with the computer program, CAST. Pockets in 1azx I and L were computed after removing the pentasaccharide from the PDB file. All volumes are in Å^3. The 2ant I model structure contains residues 1–29 and 43–432. The 2ant L structure contains residues 7–26, 43–395, and 405–432 (30). These structures were analyzed directly from the coordinates in the PDB file.

	Total[a]	H-B region[b]	Excluding 4-Å probe[c]
2ant I	4750	723	2500
1azx I	4443	1523	1954
2ant L	3984	745	2269
1azx L	5402	1138	1801

[a] The total volume of water-permeable pockets was calculated by adding the volumes of each individual pocket identified and measured using a probe with radius = 1.4 Å.

[b] The volume of pockets in the heparin-binding region (H-B) was calculated by adding the volumes of all pockets containing atoms from residues known to be implicated in direct heparin binding (15).

[c] The volume of pockets permeable to water but excluding probes with radius ≥ 4 Å. The difference in the total volumes indicates that some of the water-permeable pockets have openings or mouths, with area $>\pi$ (4 Å)^2.

TABLE IV

Pockets in the heparin-binding region of antithrombin conformers

Shape determinants in the heparin-binding region were evaluated by analyzing the distribution of key heparin-binding residues among the water-permeable pockets of free and bound antithrombin conformers. Heparin-binding pockets are those containing atoms from residues previously implicated in heparin binding on the basis of mutational analyses and published by others (15). Pockets are ranked according to volume. Heparin-binding residues contributing atoms are included in parenthesis for each pocket. Note the differences in both the volume and the residue distribution in H-B pockets in the bound *versus* the free conformer.

Rank	Volume	
	2ant I	1azx I
	Å^3	
1	251 (Arg^{129}, Arg^{132})	1192 (Arg^{132}, Arg^{145})
2	209 (Arg^{145})	81 (Arg^{24}, Glu^{113})
3	114 (Arg^{13})	78 (Arg^{145})
4	76 (Arg^{13})	60 (Lys^{11}, Asn^{45}, Lys^{125})
5	34 (Lys^{114})	58 (Lys^{125}, Arg^{129}, Arg^{132})
6	16 (Arg^{13}, Lys^{125})	33 (Arg^{145})
7	15 (Arg^{24})	12 (Lys^{125})
8	9 (Arg^{13})	8 (Arg^{145})

difference between bound and unbound conformers was obtained by assuming that the volume displaced upon heparin binding is similar to the difference in the heparin pockets' volumes in free *versus* bound conformers. Using this assumption, the estimated hydration volume change upon binding is 1100 Å^3, corresponding to ~36 water molecules. Considering only the volumes in pockets that exclude the 4-Å probe, the difference is 45 water molecules.

DISCUSSION

Conformational transitions between different functional states of proteins in aqueous solutions are linked to water transfer either from the protein to bulk solution or from bulk to the protein (20–27). The osmotic stress technique provides a thermodynamic measurement of the changes in hydration associated to the transition. Measurement of hydration changes during biological reactions is important both for understanding mechanisms and predicting reactants' behavior in hydrated biological matrixes that are subjected to osmotic forces (12, 23, 26, 27, 44).

In the present studies, osmotic stress was exploited to analyze functional hydration changes in antithrombin during binding to heparin. Osmotic stress shifted the equilibrium of the antithrombin/heparin interaction toward complex formation. The free energy change decreased linearly with the osmotic pressure induced by probes excluded from the water-permeable spaces of antithrombin. Using a small osmotic probe with ~4-Å radius, we measured transfer of ~100 water molecules from reactants to bulk upon formation of the complex.

The volumes measured increased with the size of the probe up to probes with radius of ~17 Å. This result was as expected from geometrical consideration of the solution volumes excluded by the probes. For probes smaller than the protein-heparin complex, the volume of excluded spaces increases with probe size. Large probes are completely excluded from all protein spaces as well as from all the spaces that may be defined by antithrombin and heparin during their association in the initial encounter complex.

The experimentally observed linearity of difference in ΔG with π indicates that the difference in the excess amount of water between the two states of antithrombin is well defined and remains constant within the range of the cosolute concentration used. However, several factors can contribute to nonlinearity at higher solute concentrations (27). First, for any given set of conditions, the experimentally accessible differ-

ences in ΔG, reflecting the work of water transfer, have a finite value and increasing osmotic pressure would not detect changes beyond this value. For example, whereas a decrease in K_d from 20 to 10 nM could be detected, an additional decrease from 10 to 5 nM would fall below the experimental resolution of K_d determinations. Second, increasing the osmotic pressure may eventually distort the protein's structure and change the hydration volumes of the initial and/or final states. Third, at very high concentrations, the cosolute may interact directly (*i.e.* bind) with the macromolecule surface, displacing some of the hydration waters. For these reasons, and to better approach the dilution assumptions implicit in solution theory, osmotic stress measurements are best restricted to low cosolute concentrations.

The effect of osmotic stress on the heparin/antithrombin interaction was independent of the probes' chemical characteristics. Osmotic pressure induced with polyethylene glycol, dextran, or polyvinylpyrrolidone decreased the interaction's free energy change and the transfer volumes calculated from the respective $\Delta(\Delta G)/\pi$ ratios were similar. This indicates that N_{ew}^{FB}, the difference in the number of water between the F and B state, represents a real physical volume with structural meaning. The result also indicates that other possible secondary effects of polymers, such as polymer/protein binding and changes in solution properties such as viscosity and/or dielectric constant, did not contribute significantly to the observed difference in free energy change. Although the possibility of binding interactions between cosolute and antithrombin cannot be strictly excluded, the data indicate that if there is binding, it does not differ between the F and B state.

The exclusive dependence of observed effects on osmotic stress was also demonstrated by rate measurements in binary mixtures of probes with radii of 4 and 17 Å. In the presence of a 20–200-fold molar excess of PEG 300 (~4-Å radius), effects on reaction rates measured with PEG 3400 (~17-Å radius) were not significantly different from effects measured in solutions without PEG 300. This result excluded the possibility both that the differential effects between the large and small PEG probes are due the dielectric constant of the solution and that they are related to a preferential binding interaction between the antithrombin-heparin complex and PEG.

The effect of osmotic stress on the dissociation constant was influenced by the solution's ionic strength, consistent with the previously demonstrated electrostatic nature of the antithrombin/heparin interaction (16–18, 43). At low ionic strength, the forward association rate is very fast approaching the collision limit (43). Under these circumstances, the OS effect in this reaction step is muted and the kinetically determined dissociation constant increases relative to that measured in control solutions. We interpret this observation to indicate that OS, particularly when induced with large probes, accelerates the rate at which antithrombin and proteinase surfaces approach. This approach either corresponds to or precedes the first-order rate inhibitory step, k, and is mechanistically linked to heparin dissociation (17). Thus, the dissociation rate and the K_d value, increase in stressed relative to nonstressed solutions.

The volume differences measured by computational geometry in the conformers are qualitatively consistent with the actual transfer volumes calculated from the sensitivity of K_d to water activity. Approximately one third of the volume transfer can be accounted for by differences in the volume of water-permeable pockets containing atoms from residues implicated in heparin binding. However, with a probe of radius ~4 Å, the volume differences measured in the structures correspond to ~55 fewer water molecules than the volume measured in solution by OS. The difference suggests that not all the spaces excluding cosolute during the reaction are included in the x-ray models. The additional volumes may reflect heparin hydration and/or solvent spaces defined by antithrombin and heparin in the initial complex, consistent with the observed correlation between probe size and volume transfer up to probes with sizes similar to, or larger than, antithrombin.

The difference between the volumes measured by OS and computational geometry in the x-ray-derived structures may also reflect experimental and modeling biases. For example, the volumes excluded by the probe are calculated on the assumption that the polymer behaves as a solid sphere, whereas polymers in solution are more like randomly coiled structures (40). In addition, biases in the volume and shape of water-permeable spaces may have been introduced during analyses of x-ray diffraction patterns to model the structures. This applies in particular to the 2ant model structures where some key residues are not resolved (29, 30). Another possibility is that the bound and free conformations in the crystal do not correspond to the initial and final functional conformations of bound and free antithrombin in solution. The models may simply reflect the more populated conformations under the conditions used to generate the crystals. In this regard, we should note that the structures used for analytical computational geometry in this study are derived from crystals formed under OS ($\Delta\pi \sim$ 4 atm) and include nonphysiologic molecular contacts between the loop inserted and loop exposed conformers (29, 30).

Nevertheless, the observed qualitative correlation between the functionally measured volumes and the water-permeable pockets in the structures is very significant and consistent with a heparin-induced transition between two states with different hydration volumes. Osmotic stress simply slows or accelerates reactions predetermined by the protein's structural design but does not override the conformational pathways triggered by heparin.

Taken together, the results presented in this paper demonstrate that formation of the functional complex between the sulfated GAG heparin and the serine proteinase inhibitor antithrombin is linked to net water transfer from reactants to bulk solution. The transfer volumes measured correlate with volume differences in the water-permeable pockets of x-ray-derived models of free and bound antithrombin conformers. The observed sensitivity of the heparin/antithrombin interaction to osmotic stress also indicates that the function of GAGs can be locally regulated by the osmotic potentials that maintain hydration volumes of extracellular gel matrix *in vivo*.

REFERENCES

1. Jordan, R. E., Oosta, G. M., Gardner, W. T., and Rosenberg, R. D. (1980) *J. Biol. Chem.* **255,** 10081–10900
2. Gettins, P. G. W., Patston, P. A., and Olson, S. T. (1996) *Serpins: Structure, Function and Biology*, R. G. Landes, Austin, TX
3. Carrell, R. W., Evans, D. L., and Stein, P. (1991) *Nature* **353,** 576–579
4. Lane, D. A., Olds, R. R., and Thein, S. L. (1992) *Blood Coagul. Fibrinolysis* **3,** 315–341
5. Stratikos, E., and Gettins, P. G. (1999) *Proc. Natl. Acad. Sci. U. S. A.* **96,** 4808–4813
6. Lawrence, D. A. (1997) *Nat. Struct. Biol.* **4,** 339–341
7. Huntington, J. A., Olson, S. T., Fan, B., and Gettins, P. G. (1996) *Biochemistry* **35,** 8495–8503
8. Desai, U. R., Petitout, M., Bjork, I., and Olson, S. (1998) *Biochemistry* **37,** 13033–13041
9. Rosenberg, R. D., and Lam, L. (1979) *Proc. Natl. Acad. Sci. U. S. A.* **76,** 1218–1222
10. Lindahl, U., Backstrom, G., Thunberg, L., and Leder, I. G. (1980) *Proc. Natl. Acad. Sci. U. S. A.* **77,** 6551–6555
11. Parthasarathy, N., Goldberg, I. J., Silvaram, P., Mulloy, B., Frory, D. M., and Wagner, W. D. (1994) *J. Biol. Chem.* **269,** 22391–22396
12. Tanaka, T. (1980) *Sci. Am.* **244,** 110–123
13. Futamura, A., and Gettins, P. G. (2000) *J. Biol. Chem.* **275,** 4092–4098
14. Beauchamp, N. J., Pike, R. N., Daly, M., Butler, L., Makris, M., Dafforn, T. R., Zhou, A., Fitton, H. L., Preston, F. E., Peake, I. R., and Carrell, R. W. (1998) *Blood* **92,** 2696–2706
15. Ersdal-Badju, E., Lu, A., Zuo, Y., Picard, V., and Bock, S. C. (1997) *J. Biol. Chem.* **272,** 19393–19403
16. Meagher, J. L., Beechem, J. M., Olson, S. T., and Gettins, P. G. (1998) *J. Biol.*

Chem. **273,** 23283–23289
17. Craig, P. A., Olson, S. T., and Shore, J. D. (1989) *J. Biol. Chem.* **264,** 5452–5461
18. Olson, S. T., Bjork, I., and Shore, J. D. (1993) *Methods Enzymol.* **222,** 525–559
19. Liang, J., and McGee, M. P. (1998) *Biophys. J.* **75,** 573–582
20. Colombo, M. F., Rau, D. C., and Parsegian, V. A. (1992) *Science* **256,** 655–659
21. Rand, R. P. (1992) *Science* **256,** 618
22. Colombo, M. C., and Bonilla-Rodriguez, G. O. (1996) *J. Biol. Chem.* **271,** 4895–4899
23. Douzou, P. (1994) *Proc. Natl. Acad. Sci. U. S. A.* **91,** 1657–1661
24. McGee, M. P., and Teushler, H. (1995) *J. Biol. Chem.* **270,** 15170–15174
25. Parsegian, V. A., Rand, R. P., and Rau, D. C. (1995) *Methods Enzymol.* **259,** 43–94
26. Dzingeleski, G. D., and Wolfenden, R. (1993) *Biochemistry* **32,** 9143–9147
27. Parsegian, V. A., Rand, R. P., and Rau, D. C. (2000) *Proc. Natl. Acad. Sci. U. S. A.* **97,** 3987–3992
28. Lee, K. N., Im, H., Kang, S. W., and Yu, M.-H. (1998) *J. Biol. Chem.* **273,** 2509–2513
29. Jin, L., Abrahams, J. P., Skinner, R., Petitou, M., Pike, R. N., and Carrell, R. W. (1997) *Proc. Natl. Acad. Sci. U. S. A.* **94,** 14683–14688
30. Skinner, R., Abrahams, J. P., Whisstock, J. C., Lesk, A. M., Carrell, R. W., and Wardell, M. R.(1997) *J. Mol. Biol.* **266,** 601–609
31. Skinner, R., Chang, W. S. W., Jin, L., Pei, X., Huntington, J. A., Abrahams, J. P., Carrell, R. W., and Lomas, D. A. (1998) *J. Mol. Biol.* **283,** 9–14
32. McGee, M. P., and Li, L. C. (1991) *J. Biol. Chem.* **266,** 8079–8085
33. Glasstone, S., Laidler, K., and Eyring, H. (1941) *The Theory of Rate Processes*, McGraw-Hill Inc., New York
34. Wannier, G. H. (1987) *Statistical Physics*, pp. 336–383, Dover Publications, New York
35. Joos, G., and Freeman, I. M. (1986) *Theoretical Physics*, pp. 543–552, Dover Publications, New York
36. Liang, J., Edelsbrunner, H., and Woodward, C. (1998) *Protein Sci.* **7,** 1884–1897
37. Liang, J., Edelsbrunner, H., Fu, P., Sudhakar, P., and Subramanian, S. (1998) *Proteins* **33,** 1–29
38. Kuga, S. (1981) *J. Chromatogr.* **206,** 449–461
39. Atha, D. H., and Ingham, K. C. (1981) *J. Biol. Chem.* **256,** 12108–12117
40. Knoll, D., and Hermans, J. (1983) *J. Biol. Chem.* **258,** 5710–5715
41. Arakawa, T., and Timasheff, S. N. (1985) *Biochemistry* **24,** 6756–6762
42. Connolly, T. (1983) *J. Appl. Crystallogr.* **16,** 548–558
43. Olson, S. T., Srinivasan, K. R., Bjork, I., Shore, J. D. (1981) *J. Biol. Chem.* **256,** 11073–11079
44. Maroudas, A., Wachtel, E., Grushko, G., Katz, E. P., Wainberg, P. (1991) *Biochim. Biophys. Acta* **1093,** 285–294
45. Parsegian, V. A., Rand, R. P., Fuller, N. L., and Rau, D. C. (1986) *Methods Enzymol.* **227,** 401–408